04

Instability development in the Bursian diode

© V.I. Kuznetsov, V.Yu. Koekin, M.A. Zakharov, I.K. Morozov

Ioffe Institute,
194021 St. Petersburg, Russia
e-mail: victor.kuznetsov@mail.ioffe.ru

Received July 24, 2024
Revised August 16, 2024
Accepted August 18, 2024

Stability features of a Bursian diode (a vacuum diode with an electron beam) steady states in a mode with a negative potential difference between the collector and the emitter has been studied. Using linear theory, it is shown that solutions corresponding to the middle (overlap) branch are aperiodically unstable. The development of this instability at the nonlinear stage has been numerically investigated by a high-precision E,K- code. It turned out that, depending on the phase of the perturbation, the process develops in opposite directions, and ends in stationary states lying on different branches of solutions. The process reaches solutions from the lower (normal) branch in an aperiodic manner, with a growth rate that matches the one predicted by linear theory. On the other hand, stationary solutions with reflection are affected by the process in an oscillatory manner. A general expression is obtained for the law of conservation of energy in the diode — external circuit system. In calculations of instability development, this law was carried out with high accuracy.

Keywords: Bursian diode, emitter, instability.

DOI: 10.61011/TP.2024.11.59745.239-24

Introduction

The electron flow in the Bursian diode enters the vacuum gap from an emitter with a velocity distribution function (VDF) close to monokinetic, and has a finite average velocity [1]. The system of equations describing the stationary states of a diode may have several solutions in a certain range of current densities j_0 at a fixed value j_0. This result was first obtained in Ref. [2]. Bursian diode solutions and their stability have been studied for more than 100 years (see, for example, [3–7] and references in them). The stationary solutions are conveniently represented by points on the plane $\{\varepsilon_0, \delta\}$ with a fixed potential difference between the collector and the emitter U , where ε_0 and δ — dimensionless electric field strength at the emitter and interelectrode the distance (see, for example, [7]). These points fall on continuous lines (branches of solutions). There are three branches: the lower branch (normal), the middle branch (overlap) and the upper branch with electron reflection from the virtual cathode (VC) (Fig. 1).

Solutions belonging to the normal branch are stable with respect to small perturbations and the overlap branches are aperiodically unstable in accordance with linear theory [8]. To date, linear theory has not yet been created for solutions with reflection.

We numerically study in this paper how the perturbation of solutions from the unstable branch of the overlap develops, and determine in which states the non-stationary process ends. We use high-precision E,K- code for this purpose [9]. It is shown that the process at the initial stage develops in accordance with the prediction of linear theory, and the amplitude of the disturbance changes exponentially [8]. However, the process proceeds in different directions depending on the phase of the perturbation, and it ends with a stationary solution either from the normal branch or from the branch with electron reflection. Both end states coincide with the previously found stationary solutions with high accuracy.

It was shown in Ref. [10] that the stable states of the diode can be unstable in the mode with $U < 0$ if inductance is included in the external circuit. Next, it is necessary to find out how instability develops at the nonlinear stage, as well as in what states this process will end. We study in this paper the stability of the states of these modes without reactive external load, examine the nonlinear stage of instability development and find out in what state this process ends. Simultaneously, we propose a form of the law of conservation of energy in the diode — external circuit system, and demonstrate the fulfillment of this law during calculations.

1. Stationary solutions

We consider a diode of flat geometry. The electrodes are spaced from each other at a distance of d. We believe that electrons enter the plasma from the left electrode with an average velocity of $\overline{v}_0 > 0$ and a density of n_0. The particles move without collisions, and when they reach any electrode, they are absorbed on it. We use dimensionless quantities for the convenience of consideration, choosing the electron energy at the left boundary $W_0 = m\overline{v}_0^2/2$ and the Debye Huckel length $\lambda_D = \left[2\tilde{\epsilon}_0 W_0/(e^2 n_0)\right]^{1/2}$ as units of energy and length (here e, m — the charge and mass of the electron, and $\tilde{\epsilon}_0$ — the permittivity of the vacuum).

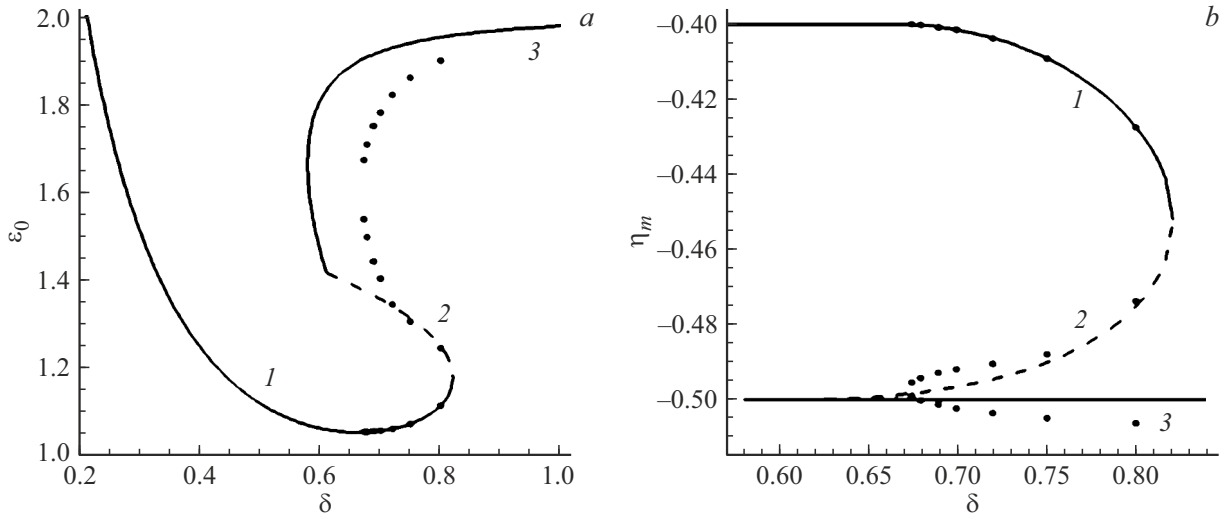

Figure 1. Dependence of the electric field strength at the emitter (a) and the minimum potential at PD (b) on the magnitude of the interelectrode distance. Solid lines — monokinetic VDF, dots — VDF in the form of „gates“ with spread $\Delta = 0.01$. *1* — normal branch, *2* — overlap branch, *3* — branch with electron reflection. $V = -0.4$.

We have for dimensionless coordinates, potential, electric field strength, velocity and time: $\xi = z/\lambda_D$, $\eta = e\Phi/(2W_0)$, $\varepsilon = eE\lambda_D/(2W_0)$, $u = v/\overline{v}_0$, $\tau = t/(\lambda_D/\overline{v}_0)$. The distance between the electrodes is $\delta = d/\lambda_D$, and the potential difference is $V = eU/(2W_0)$.

The VDF and the electron density at the point ξ is calculated in accordance with Ref. [11]. We mentally divide the VDF at the emitter $f_0(u_0)$ into groups of particles with velocities lying in a narrow range $(u_0, u_0 + \Delta u_0)$. We will call these groups „beams“ for brevity sake. The density $\Delta n(\xi; u_0)$ and the characteristic velocity $u(\xi; u_0)$ of the beam at a point with a potential $\eta(\xi)$ are expressed in terms of the corresponding values at the emitter ($\xi = 0$) by simple formulas in the collisionless case. In this case, $\Delta n(\xi; u_0)$ and $u(\xi; u_0)$ are expressed in terms of $\eta(\xi)$, and they are additionally expressed through extremes on the potential distribution (PD) in the case of particle reflection. It only remains to perform summation (integration) for all bundles that can hit the point ξ for calculating the density of the entire flow. It should be noted that not all particles came from the left electrode will be able to reach the point ξ: if the initial energy of the particle $u_0^2/2$ turns out to be less than $|\eta(\xi)|$, such a particle will be reflected at a point lying to the left of the point ξ.

Using the laws of conservation of the number of electrons for each beam (collisionless mode!)

$$\Delta n(\xi; u_0)\, u(\xi; u_0) = \Delta n(0; u_0)\, u(0; u_0) \equiv f_0(u_0)\, u_0\, \Delta u_0 \tag{1}$$

and energy for the electron

$$\frac{1}{2}u^2(\xi;\, u_0) - \eta(\xi) - \frac{1}{2}u_0^2 = 0, \tag{2}$$

we find the density of the beam at the point ξ:

$$\Delta n(\xi;\, u_0) = \frac{f_0(u_0)\, u_0\, \Delta u_0}{\left[u_0^2 + 2\eta(\xi)\right]^{1/2}}. \tag{3}$$

After performing integration over the velocity regions on the left boundary corresponding to the particles falling at the point ξ, we obtain the total density of particles at this point

$$n(\xi; u_0) = \sum_{i=0,1} \int_{\Omega_i} \frac{f_0(u_0)\, u_0\, du_0}{\left[u_0^2 + 2\eta(\xi)\right]^{1/2}}. \tag{4}$$

$i = 0$ and 1 in (4) corresponds to particles arriving at the point ξ with positive and negative velocities. The integration regions at the emitter Ω_i are determined by the type of potential distribution. It should be noted that these integrals are taken analytically for a broad class of VDF on the emitter [11,12]. Similar formulas can be obtained for any VDF moments.

We obtain the following expression for the electron density for the case when the VDF of the entering electrons is a δ-function [7]:

$$n_e(\eta; r) = \alpha(r,\, \xi_m)\,(1 + 2\eta)^{-1/2},$$

$$\alpha(r,\, \xi_m) = \begin{cases} 1 + r, & \xi < \xi_m, \\ 1 - r, & \xi > \xi_m. \end{cases} \tag{5}$$

Here ξ_m — the position of the VC point η_m. If the initial electron energy is greater than $|\eta_m|$, there are no reflected electrons, $r = 0$, and $\alpha(r, \xi_m) = 1$. The process of reflection of electrons from VC is described using the monoenergetic VDF $f_0(u_0)$ by introducing the electron reflection coefficient r which represents the fraction of the electron flow returned to the emitter ($0 \le r \le 1$). The possibility of splitting the electron beam at the reflection

point is justified by the fact that in real devices, the electrons coming from the emitter always have a small spread in velocities. Then electrons whose energies at the emitter are slightly greater than the value of the potential barrier $|\eta_m|$ overcome it, and electrons with energies slightly less than this value are reflected. Bursian introduced the electron reflection coefficient to quantify the partial reflection of electrons from VC in a stationary mode [2]. Then the dimensionless current density per collector, i.e. the fraction of the electron flow that has passed beyond the reflection point, is $j = 1 - r$. If the value is $|\eta_m| < 1/2$, the reflection coefficient is $r = 0$.

Substituting the density of electrons (5) into the Poisson equation

$$\eta'' = n_e(\eta; \eta_m) \tag{6}$$

with boundary conditions

$$\eta(0) = 0, \quad \eta(\delta) = V, \tag{7}$$

and solving this problem, we find the distributions of the potential $\eta(\xi)$ and the electric field $\varepsilon(\xi)$ in the diode. It should be noted that this problem may have several solutions for the same value δ due to the nonlinearity of the equation (6) and setting Dirichlet boundary conditions (but, of course, for different values of ε_0).

The following formulas are obtained for calculation of stationary solutions for monoenergetic VDF [7]. The PD in the region $\eta < 0$ turn out to be symmetric with respect to the position of the minimum point ξ_m in reflection-free mode. Its coordinates are expressed in terms of the electric field strength at the emitter ε_0:

$$\eta_m = \frac{1}{8}\varepsilon_0^2(4 - \varepsilon_0^2), \quad \xi_m = \frac{1}{3}\varepsilon_0(3 - \varepsilon_0^2). \tag{8}$$

For the mode without reflection of electrons in the calculations of the characteristics of stationary solutions, it is convenient to use the parameter τ — the time of electron flight from the emitter to the point ξ:

$$\xi = \frac{1}{6}\tau^3 - \frac{1}{2}\varepsilon_0\tau^2 + \tau, \quad u = \frac{1}{2}\tau^2 - \varepsilon_0\tau + 1,$$

$$\eta = \frac{1}{2}(u^2 - 1), \quad \varepsilon = \varepsilon_0 - \tau. \tag{9}$$

The following formulas are available for τ (for the overlap branch — they are marked with the symbol O, for normal — N):

$$\tau_O = 2\left[2\left(1 + \sqrt{1 + 2\eta}\right)\right]^{1/2} \cos\frac{\alpha - \pi}{3},$$

$$\tau_N = 2\left[2\left(1 + \sqrt{1 + 2\eta}\right)\right]^{1/2} \cos\frac{\alpha + \pi}{3}. \tag{10}$$

Here

$$\cos(\alpha) = -\frac{q}{2(-p/3)^{3/2}} = -\frac{6\xi}{\left[2\left(1 + \sqrt{1 + 2\eta}\right)\right]^{3/2}}, \tag{11}$$

and the parameters q and p are the coefficients of the cubic equation $x^3 + px + q = 0$, to which the 1st equation (9) is reduced, and are equal to: $q = 12\xi$, $p = -6\left(1 + \sqrt{1 + 2\eta}\right)$ (see, for example, [13]).

In the electron reflection mode (Fig. 1, curve *3*) it is convenient to use the reflection coefficient r as a parameter, which varies from 0 to 1 on this branch. In contrast to the case when there are no reflected electrons ($r = 0$), the PD in the region $\eta < 0$ turn out to be asymmetric relative to the reflection point ξ_r in the mode with reflection. The following parameter values correspond to this point:

$$\varepsilon_0 = \sqrt{2(1 + r)}, \quad \xi_r = \frac{1}{3}\sqrt{\frac{2}{1 + r}}, \quad \eta_r = -\frac{1}{2}. \tag{12}$$

To the left of the point ξ_r

$$\eta(\xi) = -\frac{1}{2} + \frac{1}{2}\left(1 - \frac{\xi}{\xi_r}\right)^{4/3}, \quad \varepsilon(\xi) = \frac{2}{3\xi_r}\left(1 - \frac{\xi}{\xi_r}\right)^{1/3}, \tag{13}$$

and to the right of it —

$$\eta(\xi) = -\frac{1}{2} + \frac{1}{2}\left(\frac{1 - r}{1 + r}\right)^{2/3}\left(\frac{\xi}{\xi_r} - 1\right)^{4/3},$$

$$\varepsilon(\xi) = \frac{2}{3\xi_r}\left(\frac{1 - r}{1 + r}\right)^{2/3}\left(\frac{\xi}{\xi_r} - 1\right)^{1/3}. \tag{14}$$

Stationary solutions are conveniently represented by points on the plane (ε_0, δ). These points form separate curves with a fixed value of the potential V, which are called branches of solutions [9]. These branches for the case of a monoenergy VDF are shown by solid curves in Fig. 1.

Now let us consider the case when the electron flow has a VDF in the form of „gates“

$$f_0(u_0) = (2\Delta)^{-1}\Theta\left[\Delta^2 - (1 - u_0)^2\right]. \tag{15}$$

Here $\Theta(x)$ — Heaviside function. It is equal to one with $x \geq 0$ and 0 with $x < 0$. We will use such a VDF of electrons at the emitter in numerical calculations of the instability development process.

In the mode without reflection of electrons, the potential in the minimum is $\eta_m > -(1 - \Delta)^2/2$, and all electrons flying out from the left boundary reach the opposite electrode. η_m changes in the interval $[-(1 + \Delta)^2/2, -(1 - \Delta)^2/2]$ in reflection mode. The reflection of electrons begins at the point $\xi_- < \xi_m$, where the potential $\eta = -(1 - \Delta)^2/2$ (ξ_m — the position of the minimum of PD). There are both electrons that flew out from the left electrode and moving to the right boundary, and electrons reflected from the barrier in the section (ξ_-, ξ_m) in the section $(0, \xi_-)$. A flow of reflected electrons is formed at this section. Only electrons that have overcome the potential minimum η_m and are moving to the right electrode are present in section (ξ_m, δ). The following expressions are obtained using the

formula (4) for the electron density [9]:

$$n_e(\eta, \eta_m) = \frac{1}{2\Delta}\begin{cases} \sqrt{(1+\Delta)^2+2\eta} - \sqrt{(1-\Delta)^2+2\eta}, \\ \qquad \eta_m > -\frac{1}{2}(1-\Delta)^2 \\ \sqrt{(1+\Delta)^2+2\eta} + \sqrt{-2\eta_m+2\eta} \\ \qquad -2\sqrt{(1-\Delta)^2+2\eta}, \\ \qquad \xi < \xi_m, \eta > -\frac{1}{2}(1-\Delta)^2, \\ \sqrt{(1+\Delta)^2+2\eta} + \sqrt{-2\eta_m+2\eta}, \\ \qquad \xi < \xi_m, \eta < -\frac{1}{2}(1-\Delta)^2, \\ \sqrt{(1+\Delta)^2+2\eta} - \sqrt{-2\eta_m+2\eta}, \\ \qquad \xi > \xi_m. \end{cases} \tag{16}$$

All PD can be found after substituting the concentration (16) into the Poisson equation (6) and the use of boundary conditions (7). Their structure is described in detail in Ref. [9]. Solutions are shown by bold dots in Fig. 1. It can be seen that the solution branches do not differ much from the corresponding branches for the case of a monokinetic VDF. However, now some of the solutions on the overlap branch turn out to be solutions with electron reflection (for those values ε_0, which correspond to PD with $\eta_m < -(1-\Delta)^2/2$) (Fig. 1, *b*). Solutions, as in the case of monokinetic VDF, are determined by three dimensionless parameters: the interelectrode distance $\delta = d/\lambda_D$, the potential difference between the electrodes $V = eU/(2W_0)$ and the electric field strength at the left electrode ε_0. However, they are also slightly affected by the speed variation Δ. It has a particularly strong effect on solutions with electron reflection.

It should be noted that if the spread of the VDF is small, i.e. $\Delta \ll 1$, the type of VDF inside the interval $[(1-\Delta), (1+\Delta)]$ should not affect the results of calculations of electron density distributions and fields in the interelectrode gap. That's why we chose the simplest type of VDF with a spread of energy (16).

2. Dispersion properties of plasma

When studying the dispersion properties of plasma in the mode without reflection of electrons from a potential barrier, when there are no reactive elements in the external circuit of the diode, we use the dispersion equation for monokinetic electron VDF [9]:

$$Z(\delta, \omega) = \frac{1}{\omega^4}\left[(2 - i\omega T)\exp(i\omega T) - i\omega^3\delta - i\omega T - 2\right] = 0. \tag{17}$$

This equation is obtained by the method of small perturbations: the solution of the non-stationary problem is sought by substituting PD in the following form

$$\eta(\tau, \xi) = \eta_0(\xi) + \tilde{\eta}(\xi)\exp(-i\omega\tau), \quad |\tilde{\eta}(\xi)| \ll |\eta_0(\xi)|, \tag{18}$$

in the Poisson equation and linearization of the unsteady electron density by a small perturbation $\tilde{\eta}(\xi)$. The result is a linear integral equation for the amplitude of the disturbance PD $\tilde{\eta}(\xi)$. This equation can be solved analytically for the Bursian diode [8]. After using the zero boundary condition on the collector for $\tilde{\eta}(\xi)$, the desired dispersion equation is obtained.

Solutions of the dispersion equation — these are the eigenvalues of perturbations: $\omega = \Omega + i\Gamma$, where Ω is the frequency, and Γ is the growth rate. It is known that the dispersion equation has a countable number of solutions for diodes with collisionless plasma, for each value of the interelectrode gap δ. The Bursian diode has one aperiodic and many oscillatory eigenvalues for each stationary solution. The aperiodic solution is found by substituting $\omega = i\Gamma$ into equation (17):

$$\Gamma^{-4}\left[(2 + \Gamma T)\exp(-\Gamma T) - \Gamma^3\delta + \Gamma T - 2\right] = 0. \tag{19}$$

For solutions corresponding to the normal branch, the growth rates turn out to be negative, and it is positive for the overlap branch. This suggests that solutions with an overlap branch are unstable with respect to small perturbations. It can be shown by decomposing the small Γ of the left side (19) that the growth rate vanishes at the bifurcation point $\delta_{SCL} = (\sqrt{2}/3)\left(1 + \sqrt{1+V}\right)^{3/2}$, where the normal and overlap branches meet. It is necessary to solve the complete complex equation (17) to find the oscillatory branches.

The dispersion curves, i.e. the dependences of the eigenvalues on the magnitude of the interelectrode distance, are shown in Fig. 2. The dashed curves correspond to solutions with the overlap branch (they are marked with the index „O"), and the solid curves correspond to solutions with the normal branch (they are marked with the index „N"). The aperiodic branches are marked with the letter „A", the oscillatory are marked with the letter „O". The figure shows only two oscillatory dispersion branches having the smallest (in absolute value) decrements.

It can be seen that the growth rates are negative for all oscillatory dispersion branches, i.e. the stationary solutions in the mode without reflection of electrons from the potential barrier can only be aperiodically unstable in the Bursian diode with $V < 0$ and these are solutions with overlap branches.

Currently there is no linear theory for studying the stability of solutions corresponding to the branch with reflection (curve *3* in Fig. 1), so the stability of such solutions can only be studied using numerical methods (see, for example, the paper [9]). The values of proper frequencies obtained numerically are given below for $\delta = 0.75$, $V = -0.4$.

It is interesting to trace how the process of instability development proceeds, and in what state it ends. This is addressed in sect. 3.

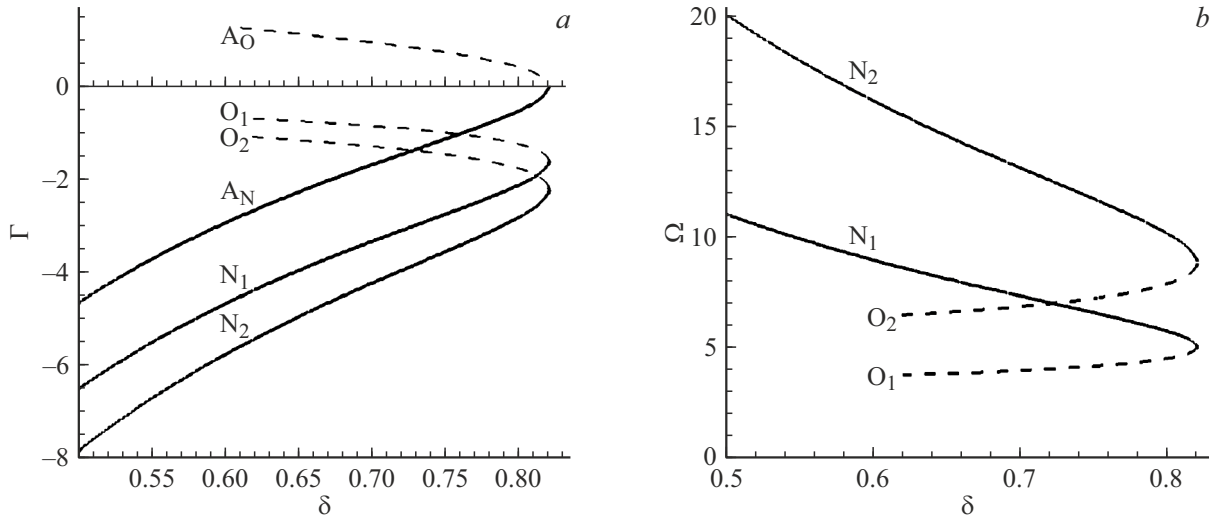

Figure 2. Growth rates (a) and frequencies (b) of the dispersion curves corresponding to the normal (solid) and overlap (dashed) branches for the monokinetic Fed. $V = -0.4$.

3. Numerical calculations of instability development processes

We carry out numerical calculations of the development of perturbation using the E,K- code. It is described in detail, for example, in Ref. [9]. The calculations used the shape of the electric field perturbation and the growth rates found by the linear theory. An unstable stationary solution on the overlap branch for $\delta = 0.75$, $V = -0.4$ was considered as an initial solution. Since the E,K-code does not provide for the use of a monokinetic VDF, it was taken in the form (16) with a spread of $\Delta = 0.01$. The considered stationary state corresponds to the mode without reflection of electrons for selected parameter values, as can be seen from Fig. 1, b ($\eta_m > -(1-\Delta)^2/2$). This figure also shows that two more stationary solutions can exist with these values of parameters: one (without reflection of electrons) lies on the normal branch (curve *1*), and the other on the branch with reflection (curve *3*). Let's see if the non-stationary process can end in any of these solutions.

The following values of space-time cells were selected in the calculations: 200 division points were taken according to the coordinate, i.e. $\Delta\xi = 0.00375$, and the time step is $\Delta\tau = 0.02$. The initial condition — the distribution of the electric field in the gap was set equal to the sum of the stationary field in the first 400 time steps and the disturbance:

$$\varepsilon(\tau,\ \xi) = \varepsilon(0,\ \xi) + a\,F(\xi)\,\exp(\Gamma\tau),$$

$$F(\xi) = -\Gamma^{-3}u(t)^{-1}\Big[(1+\Gamma t)\,\exp(-\Gamma t) + 1/2\Gamma^2 t^2 - \varepsilon_0\Gamma^2 t + \Gamma^2 - 1\Big]. \qquad (20)$$

The solid curve in Fig. 3 shows the normalized disturbances of the electric field (Fig. 3, a) and potential distributions (Fig. 3, b), while the corresponding dependences obtained in the calculations are shown by the dashed curve. It can be seen that the theoretical dependences for the monokinetic VDF and the dependences obtained in calculations for a beam with a spread are close. Here t is related to ξ formulas (9), (10); a — the amplitude of the field disturbance, and $F(\xi)$ — form factor which does not change during the initial stage of perturbation development, since the process is aperiodic. The linear theory gives an growth rate value of $\Gamma = 0.738$ for selected parameters. The magnitude of the amplitude a was assumed to be equal to 10^{-5}. The form factor $F(\xi)$ was determined by the perturbation of the electric field found by linear theory. It is shown by a solid curve in Fig. 3, and the form factor obtained in the calculations is shown by the dashed curve. It can be seen that the form factors for the monokinetic VDF and for the beam with spread are close.

The amplitude of the disturbance is determined with an accuracy of phase in the linear theory. As will be shown below, when choosing a phase equal to zero (sign „+“ for a), the process goes towards the normal branch (curve *1* in Fig. 1), and with a phase equal to π (sign „-“ for a), — towards the branch with reflection (curve *3* in Fig. 1).

Calculations have shown that if the sign „+“ is selected for the amplitude of the disturbance, the process ends with an exit to a stationary solution corresponding to the normal branch. This can be seen in Fig. 4 and 5 (curves *1*), which show the temporal evolutions of the electric field and convection current strengths at the emitter and collector, as well as in Fig. 6 (curves *1*), demonstrating the temporal evolutions of the minimum potential and its position. It is also apparent that the disturbance develops aperiodically at the initial stage. This is confirmed by the immutability of the shape of the electric field disturbance.

The high accuracy of the E,K-code allows extracting the growth rate value from the calculated process characteristics. The non-stationary dependence $f_i(\tau_i)$ was processed using

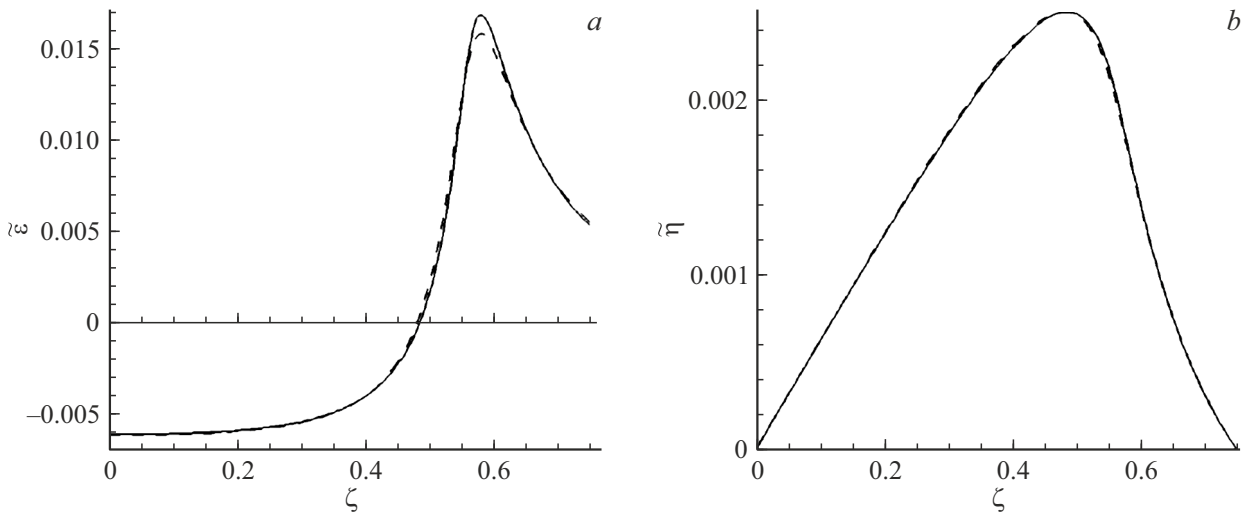

Figure 3. Perturbances of electric field distributions (a) and potential (b). The solid curve is derived from linear theory for monokinetic VDF, the dashed curve is derived from calculations for a beam with a spread of $\Delta = 0.01$. Both curves are scaled by the maximum of the PD perturbation. $\delta = 0.75$, $V = -0.4$.

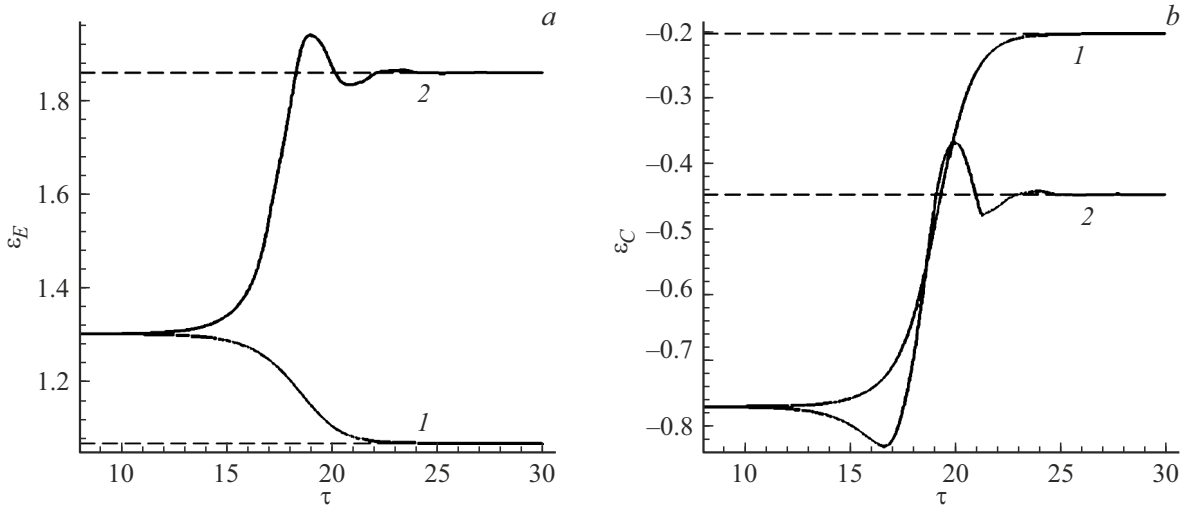

Figure 4. Time evolutions of electric field strengths at emitter (a) and collector (b) for perturbation phase 0 (*1*) and π (*2*). The dashed lines correspond to stationary solutions for $\delta = 0.75$, $V = -0.4$, $\Delta = 0.01$.

the least squares method. An approximating function of the following form was used for this purpose:

$$f(\tau) = c + [a\ \cos(\omega\tau) + b\ \sin(\omega\tau)]\exp(\Gamma\tau). \qquad (21)$$

The least squares method in this case is to minimize the functional of five variables:

$$M(c, a, b, \omega, \Gamma) = \sum_i [f_i(\tau_i) - f(\tau_i)]^2. \qquad (22)$$

The coefficients at which the minimum functional (22) were determined using the gradient descent method. The calculated growth rate turned out to be equal to 0.752, which practically coincides with the growth rate found according to linear theory using monokinetic electron VDF at the emitter ($\Gamma = 0.738$).

Fig. 4–6 shows that the process reaches a stationary solution when the perturbation has a phase equal to 0 (sign „+“ for a), and it coincides with the solution lying on the normal branch. The output occurs aperiodically. The calculations made it possible to find the value of the decrement. It turned out to be equal to -1.138 and practically coincided with the one found according to the linear theory with the monokinetic VDF of electrons at the emitter ($\Gamma = -1.133$). At the same time, both during the initial stage of perturbation development and when entering the stationary mode, the frequency obtained during processing of the process ω turned out to be zero, which corresponds to the aperiodic nature of the process.

On the other hand, when the perturbation has a phase equal to π, the process ends with a stationary solution

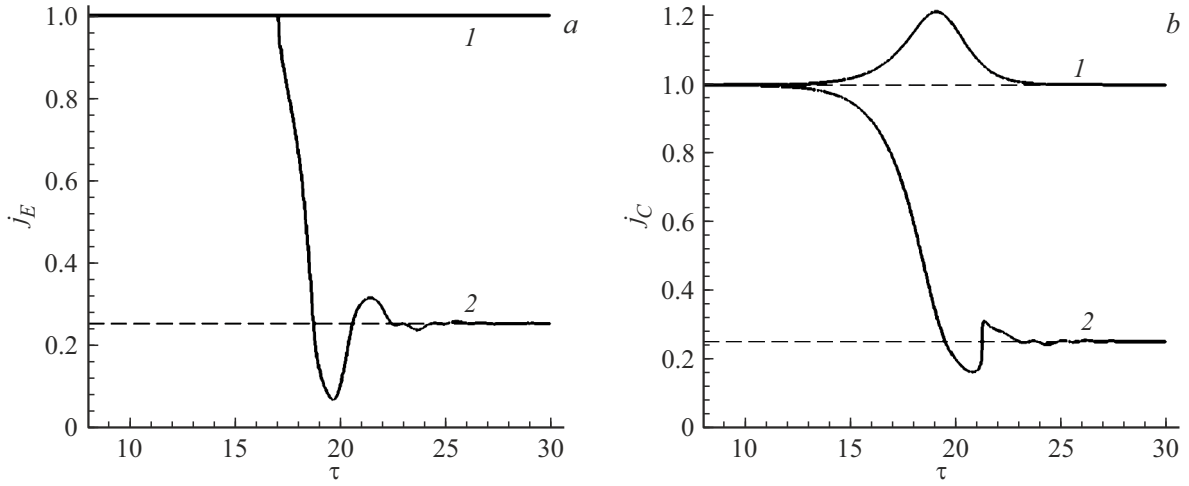

Figure 5. Time evolutions of the convection current at emitter (a) and collector (b) for perturbation phase 0 (*1*) and π (*2*). Dashed lines have the same meaning as in Fig. 4.

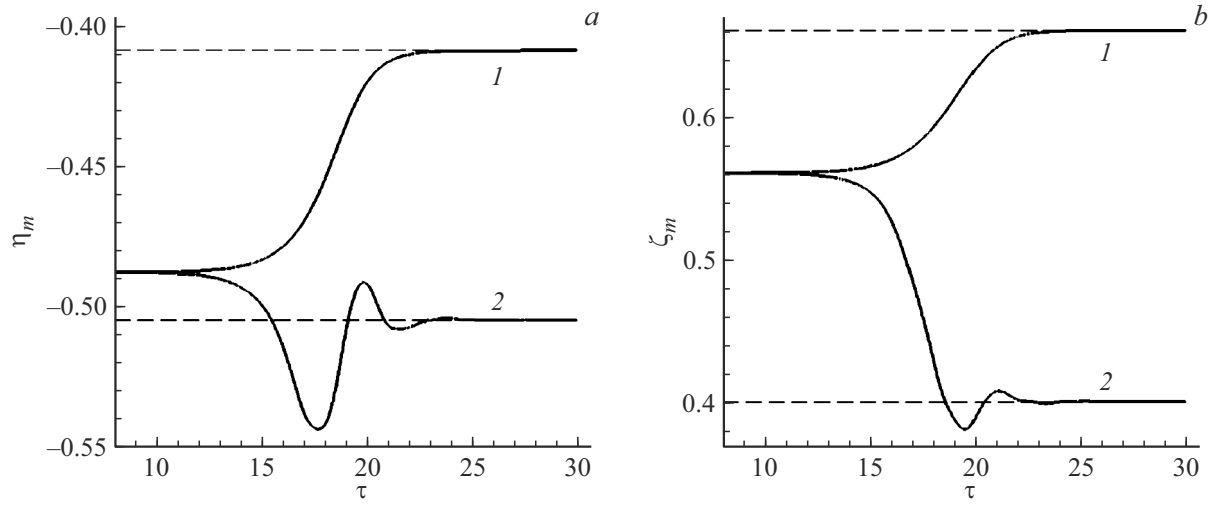

Figure 6. Time evolutions of the minimum value of the potential (a) and its position (b) for the perturbation phase 0 (*1*) and π (*2*). Dashed lines have the same meaning as in Fig. 4.

corresponding to the branch with electron reflection from the VC (branch *3* in Fig. 1). This can be seen from fig. 4 and 5, which show the temporal evolutions of the electric field and convection current strengths at the emitter and collector, as well as Fig. 6, demonstrating the temporal evolutions of the minimum potential and its position. The stationary solution with reflection is reached through damped oscillations unlike the case when the zero phase was selected and the process reached a solution without reflection of electrons. The calculations made it possible to determine the density Γ and the frequency Ω. As a result of processing the dependence of the electric field strength at the emitter on time using the least squares method, the values of these quantities turned out to be -0.43 and 5.19, respectively.

Fig. 7 shows the evolution of the potential distribution $\eta(\tau, \xi)$ and the electron density $n(\tau, \xi)$ in the interelectrode gap when the transition to the electron reflection mode occurs. When reflected particles occur, it can be seen that strong gradients appear on the particle density distribution $n(\tau, \xi)$ in the vicinity of the potential minimum. In addition, it can be seen that the density varies by more than an order of magnitude along the coordinate. It was necessary to additionally calculate the density at intermediate points of cells adjacent to the maximum density at each moment τ to ensure high accuracy of calculation $n(\tau, \xi)$.

4. Conservation laws in the diode — external circuit system

We checked the fulfillment of the laws of conservation of total current in the course of calculations, as well as energy in the diode — external circuit system.

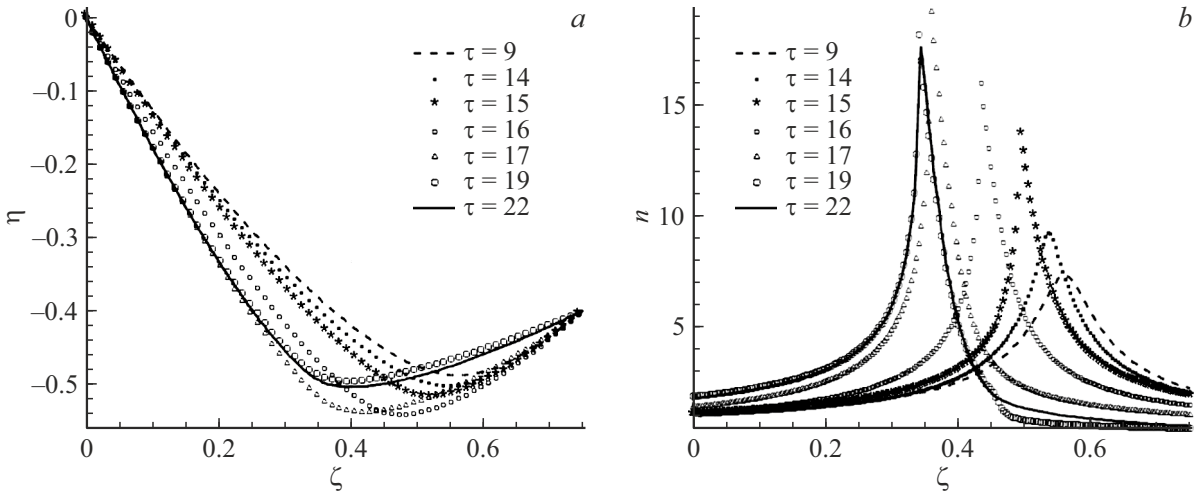

Figure 7. The evolution of potential distributions (a) and electron densities (b) during the transition to the branch with reflection for a number of time points τ. $\delta = 0.75$, $V = -0.4$, $\Delta = 0.01$.

4.1. Conservation of full current

It is known that the total current should not depend on the coordinate in a one-dimensional plasma diode. It consists of the convection current $j_{conv}(t, z)$ and the displacement current $j_{dis}(t, z)$ at every moment of time t at the gap point z:

$$j(t) = j_{conv}(t, z) + j_{dis}(t, z) = j_{conv}(t, z) + \frac{1}{4\pi}\frac{\partial}{\partial t}E(t, z). \tag{23}$$

Fig. 8 shows the evolution of the total current at the emitter and collector for cases when the process ends reaching the normal branch (Fig. 8, a) and a branch with reflection (Fig. 8, b). It can be seen that these currents coincide with a high degree of accuracy in both processes. This indicates that the numerical code works correctly.

4.2. The law of conservation of energy in the diode — external circuit system

The law of conservation of energy in a diode with a flow of charged particles is formulated as follows: the change in the total energy W_{in} in the interelectrode gap per unit of time is equal to the algebraic sum of the energy flows through the surfaces of the emitter $S_W(t, 0)$ and the collector $S_W(t, d)$, as well as the energy released to external load $P_{ec}(t)$. Let's look at these components in more detail.

The total energy W_{in} consists of the total energy of the electric field E generated by charges, W_{Ef}, and the kinetic energy of charged particles in the volume, W_{kin}:

$$W_{in} = W_{Ef} + W_{kin} = \int_0^d \frac{1}{8\pi}E^2(x)\,dx + \int_0^d w_{kin}(x)\,dx. \tag{24}$$

Charged particles inside the gap induce surface charges on the electrodes. When the particles move, the surface charges change over time, the electric field at the surface of the electrodes changes, and an electric current is induced in the external circuit. This is the displacement current j_{dis}. If the particles did not reach the electrodes (and did not come from the emitter), then a current j would flow in the external circuit, equal to j_{dis}, energy equal to $j|U|$ would be released on the external load, where U — external voltage, and energy would flow through the surfaces of the emitter and collector $-j\varphi_E$ and $j\varphi_C$, where φ_E and φ_C — the work function of the emitter and the collector. Thus, energy would be released in the external circuit in this case

$$\begin{aligned} P_{ec}(t) &= j|U| - j\varphi_E + j\varphi_C \\ &= -j(t)\,(\varphi_E - \varphi_C - |U|) = -j(t)\cdot\Phi_C. \end{aligned} \tag{25}$$

Here Φ_C — the internal potential difference between the electrodes. When flows of charged particles appear through the electrode surfaces, a convection current is additionally added to the displacement current in the external circuit, and the current flowing in the external circuit should be determined by the formula(23). As already noted, the total currents at the emitter and collector at each moment of time turn out to be the same in the one-dimensional case.

Therefore, the law of conservation of energy has the form

$$\begin{aligned} &\frac{\partial}{\partial t}\left[\int_0^d \frac{1}{8\pi}E^2(t, x)\,dx + \int_0^d w_{kin}(t, x)\,dx\right] \\ &= S_W(t, 0) + S_W(t, d) - \Phi_C\left[j_{conv}(t, d) + \frac{1}{4\pi}\frac{\partial}{\partial t}E(t, d)\right]. \end{aligned} \tag{26}$$

Let us consider the example (Fig. 9). Let an infinitely thin charged plate with charge Q be located at the point Z at the moment of time t. Let's use E_1 to denote the electric field strength to the left of the plate, and E_2 to denote the electric field strength the right of the plate. We have a system of

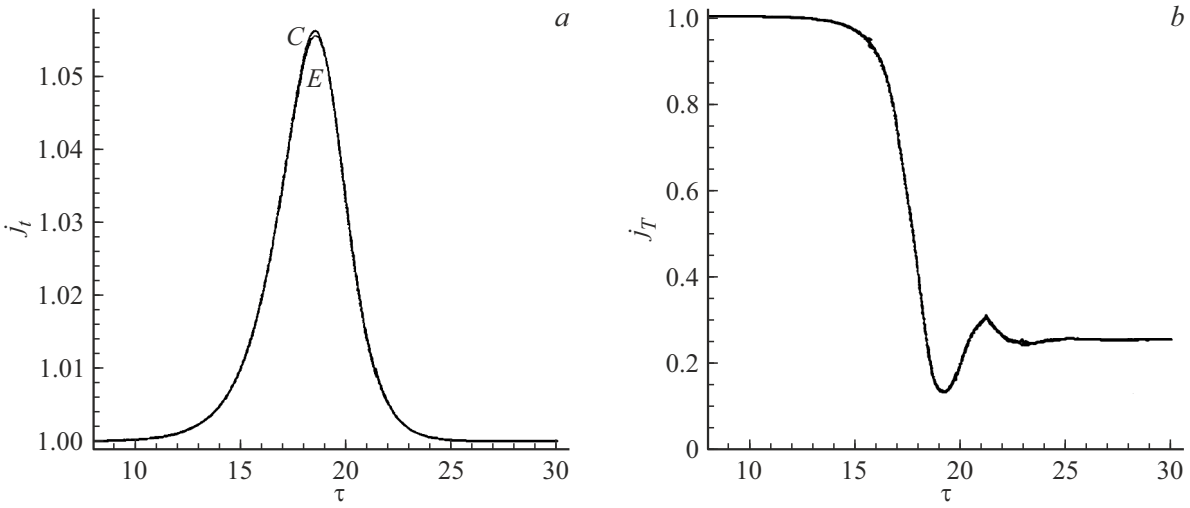

Figure 8. Time evolutions of the total current at emitter (solid curve) and collector (dotted curve) for perturbation phase 0 (a) and π (b). $\delta = 0.75$, $V = -0.4$, $\Delta = 0.01$. The curves match with a high degree of accuracy.

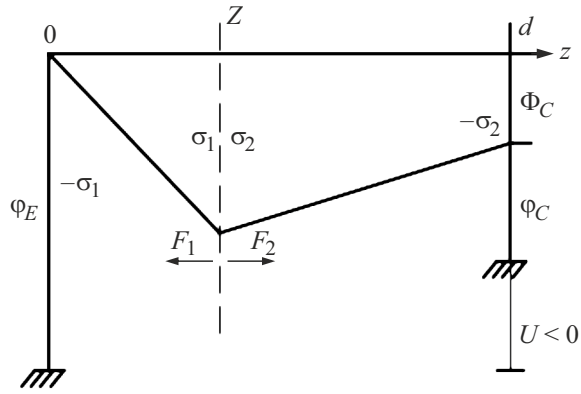

Figure 9. Forces acting on an infinitely thin charged layer when it moves in a flat diode.

equations to calculate these fields:

$$E_2 - E_1 = 4\pi Q,$$

$$E_2 (d - Z) - E_1 Z = -\Phi_C. \tag{27}$$

Its solution has the form

$$E_1 = -\frac{\Phi_C}{d} - 4\pi Q \frac{d - Z}{d},$$

$$E_2 = -\frac{\Phi_C}{d} + 4\pi Q \frac{Z}{d}. \tag{28}$$

The charge Q induces surface charges on the electrode surfaces. When the plate moves, they change over time, changing the electric fields at the electrode surfaces, and an electric current is induced in the external circuit. Since in this case there are no streams of charged particles on the surface of the electrodes, the total current in the external circuit coincides with the displacement current:

$$j(t) = \frac{1}{4\pi} \frac{\partial}{\partial t} E(t, Z) = \frac{Q}{d} v. \tag{29}$$

Let us calculate the total energy of the field in the gap and the kinetic energy of the plate. For the energy of the electric field, we obtain

$$W_{Ef} = \int_0^d \frac{1}{8\pi} E^2(x) dx = \frac{1}{8\pi} \left[E_1^2 Z + E_2^2 (d - Z)\right]$$

$$= \frac{1}{8\pi d} \left[\Phi_C^2 + 16\pi^2 Q^2 Z(d - Z)\right]. \tag{30}$$

Now let us calculate the total kinetic energy of the moving plate. A force acts on each element of the plate on the right side

$$F_2 = \frac{1}{2}\sigma_2 E_2 = \frac{1}{8\pi} E_2^2, \tag{31}$$

and on the left —

$$F_1 = \frac{1}{2}\sigma_1 E_1 = \frac{1}{8\pi} E_1^2. \tag{32}$$

Here $\sigma_{1,2}$ — the density of the surface charge to the left and right of the plate, respectively. At the same time, both of these forces are directed along the external normal to each of the surfaces of the plate (Fig. 9). Therefore, the total force acting on the charged plate is equal to

$$F = F_2 - F_1 = \frac{1}{8\pi} \left(E_2^2 - E_1^2\right) = \frac{4\pi Q^2}{d} \left(Z - \frac{d}{2} - \frac{\Phi_C}{4\pi Q}\right). \tag{33}$$

The equation of motion of the plate has the form

$$m\ddot{Z} = F = \frac{4\pi Q^2}{d} \left(Z - \frac{d}{2} - \frac{\Phi_C}{4\pi Q}\right). \tag{34}$$

By multiplying both parts of (34) by v and integrating, for the kinetic energy of the plate we obtain

$$W_{kin} = \frac{m v^2}{2} = \frac{m v_0^2}{2} - \frac{2\pi Q^2}{d} \left(\frac{d}{2} + \frac{\Phi_C}{4\pi Q}\right)^2$$

$$+ \frac{2\pi Q^2}{d} \left(Z - \frac{d}{2} - \frac{\Phi_C}{4\pi Q}\right)^2. \tag{35}$$

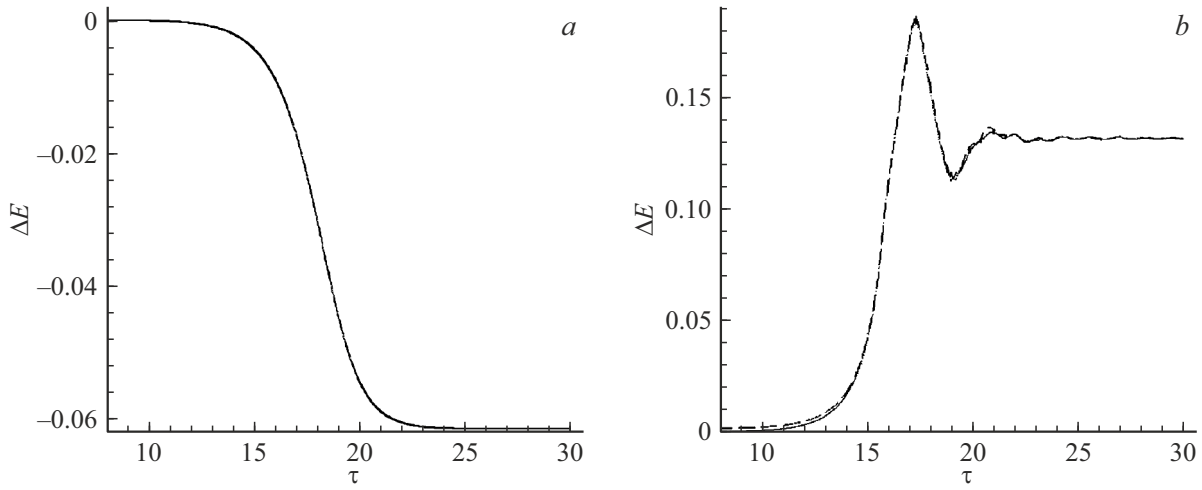

Figure 10. The law of conservation of energy during transition to normal branch (a) and to branch with reflection (b). The solid curve corresponds to the increase in total energy in the gap, the dashed curve corresponds to the sum of the energy flows to the electrodes and the energy released on the external load. $\delta = 0.75$, $V = -0.4$, $\Delta = 0.01$.

By the way, it can be seen from this expression that if Φ_C and d are fixed, then when the plate charge exceeds a certain value depending on Φ_C and d, the velocity will vanish at some point of the gap, and the plate will turn back, i.e. it will be locked by its own electric field. For instance, the value of $|Q|$ should be greater than $(m v_0^2 d/(4\pi Z(d-Z))^{1/2}$ for $\Phi_C = 0$.

The rate of change of the total energy in the gap is

$$\frac{\partial}{\partial t}(W_{Ef} + W_{kin}) = 4\pi Q^2 \left(\frac{1}{2} - \frac{Z}{d}\right) v + 4\pi Q^2 \left(\frac{Z}{d} - \frac{1}{2} - \frac{\Phi_C}{4\pi Q d}\right) v = -\frac{Qv}{d}\Phi_C = -j\Phi_C. \quad (36)$$

This expression coincides with the right-hand side of the formula (26), which confirms its correctness in the case of the absence of particle flows on the electrodes.

We calculated each of the terms of the formula (26) in each time moment. It was convenient to use the integral form of the law of conservation of energy:

$$W_{in}(t) - W_{in}(t_0) = \int_{t_0}^{t} dt' \left[S_W(t', 0) + S_W(t', d) - \Phi_C j(t', d)\right]. \quad (37)$$

Figure 10 shows the evolution of the left and right parts of the formula (37) during transitions to the normal branch (dashed curve) and to the branch with reflection (dotted curve). It can be seen that in both cases the law of conservation of energy is fulfilled with good accuracy.

Conclusion

The processes of instability development in the Bursian diode have been studied for the case when a negative potential difference is applied between the collector and the emitter. It is shown that instability develops from the state lying on the overlap branch in accordance with the linear theory. At the same time, the shape of the perturbations remains unchanged, and the growth rate is close to the theoretical one. It is also shown that, the process can have different directions and end in different states that coincide with stationary solutions depending on the sign of the amplitude of the perturbations.

The calculations were validated by checking that the total current does not depend on the coordinate, as it should be in a one-dimensional diode. The currents calculated during the calculations of the processes at the emitter and collector practically matched. An analytical expression is obtained for the law of conservation of energy in the diode — external circuit system. The correctness of the formula is confirmed by a simple example of the motion of a charged layer in an interelectrode gap. It was demonstrated by the calculations that the law of conservation of energy is fulfilled with a good degree of accuracy.

The conducted research will make it possible to further study the processes of instability development in the diode — external circuit system in the presence of reactive elements in the external circuit. The possibility of instability in the mode with $U < 0$ in the presence of inductance was discovered earlier in Ref. [10]. In contrast to the case when the external circuit has no reactive elements, the reactive load leads to the appearance of time-varying boundary conditions for the potential at the electrodes, which complicates the research. It is important to understand in which states the process of instability development will end. The results obtained may be useful in the creation of microwave radiation generators [14,15].

Funding

Sections 4, 5 of the paper were developed with the financial support of the Russian Academy of Sciences, project

No.24-22-00175; section 1–3 — within the framework of the state assignment, topic number FFUG-2024-0005.

Conflict of interest

The authors declare that they have no conflict of interest.

References

[1] M.V. Nezlin. *Physics of Intense Beams in Plasmas* (IOP, Bristol, 1993).
[2] V.R. Bursian, V.I. Pavlov. Zhurn. rus. fiz.-him. obshch-va, **55** (1-3), 71 (1923) (in Russian).
[3] C.E. Fay, A.E. Samuel, W. Shockley. Bell Syst. Tech. J. **17** (1), 49-79 (1938). DOI: 10.1002/j.1538-7305.1938.tb00775.x
[4] R.J. Lomax. Proc. Inst. Elect. Engrs. Pt.C., **108** (13), 119 (1961). DOI: 10.1049/pi-c.1961.0018
[5] V.I. Kuznetsov, A.V. Solovyov, A.Ya. Ender. Sov. Phys. Tech. Phys., **39**, 1207 (1994).
[6] P.V. Akimov, H. Schamel, H. Kolinsky et al. Phys. Plasmas., **8** (8), 3788 (2001). DOI: 10.1063/1.1383287
[7] V.I. Kuznetsov, A.Ya. Ender. Tech. Phys., **58**, 1705 (2013).
[8] V.I. Kuznetsov, A.Ya. Ender. Plasma Phys. Rep., **41** (11), 905 (2015).
DOI: https://doi.org/10.1134/S1063780X15110069
[9] V.I. Kuznetsov, A.Ya. Ender. Plasma Phys. Rep., **36** (3), 226 (2010). DOI: 10.1134/S1063780X10030049
[10] V.I. Kuznetsov, A.B. Gerasimenko. J. Appl. Phys., **125**, 183301 (2019). DOI: org/10.1063/1.5090204
[11] A.J. Ender. *Termoemissionnyj preobrazovatel' teplovoj energii v elektricheskuyu v knudsenovskom rezhime*. Kand. diss. L.: FTI im. A.F. Ioffe, 1972) (in Russian).
[12] V.I. Kuznetsov. *Issledovanie nelinejnyh nestacionarnyh processov v besstolknovitel'noj plazme, obrazuyushchejsya na poverhnosti*. Kand. diss. L.: FTI im. A.F. Ioffe, 1981) (in Russian).
[13] G. Korn, T. Korn. *Spravochnik po matematike. Dlya nauchnyh rabotnikov*, (Nauka, M., 1974) (in Russian).
[14] A.E. Dubinov, V.D. Selemir. J. Comm. Technol. Electron., **47**, 575 (2002).
[15] S.E. Mumtaz, H.S. Uhm, Eun Ha Choi. Phys. Rep., **1069**, 1 (2024). DOI: org/10.1016/j.physrep.2024.03.003

Translated by A.Akhtyamov